20% per day. It remains to be determined whether this variation can be attributed to food-web structure, the ratio of nutrients (C:N:P), or to environmental factors such as light and temperature. □

Methods

Field sampling. Methods specific to Mouse and Ranger Lake are described elsewhere[7]. Methods for the remaining 18 lakes are described below. Only lakes that had a maximum depth ≥4 m were considered, in order to minimize benthic effects on the pelagic zone (Table 1). Lakes on rivers were avoided, to limit the effects of river water on the pelagic environment. Lakes with minimal shoreline development (except Nakamun Lake) were chosen, to minimize human effects on lake nutrient cycling. Most lakes had thermally stratified water columns; however, two isothermal lakes were included from the Interior Plains (Table 1). Only lakes with total phosphorus concentrations below 100 $\mu g\, l^{-1}$ were selected. Water (20 litres) was removed at the mid-epilimnetic depth of each lake with a Van Dorn sampler and placed in 20-litre polyethylene containers (acid-washed) held in coolers. When a distinct epilimnion or mixing depth was not present, water was removed from just below the surface (≤1 m).

Laboratory methods. Detailed laboratory methods are described elsewhere[7]. Lake water was placed in 4-litre clear polyethylene containers that had been washed (0.1% contrad-70), rinsed (ethanol) and leached (0.1 M HCl). Each sample was incubated with carrier-free radiophosphate ($^{33}PO_4$; 270–2,100 Bq ml^{-1}; ICN Biomedicals) for ~27 h (range 21–47 h) to label the planktonic community. Lake water was incubated near ambient temperatures (±2 °C), which ranged from 18 to 22 °C. This range minimized the effects of temperature on rate measurements. Incubations were terminated by injection of competitive inhibitor ($^{31}PO_4$; final concentration 1–5 mg P litre^{-1}). This prevented re-incorporation of ^{33}P after it was released from the plankton. We then measured the accumulation of ^{33}P in the dissolved pool over time: the slope of this line provided an estimate of the release rate of dissolved ^{33}P. The remaining lake water was analysed for total P (ref. 22), which was calculated as the sum of dissolved and particulate P. The release rate of dissolved P was calculated by using the following formula: P release rate = ^{33}P release rate × total P/total ^{33}P, so our definition for phosphorus regeneration was the transfer of phosphorus from the particulate pool (>0.2 μm) to the dissolved pool (<0.2 μm) over time. Egestion, excretion, decay, cell lysis, cellular exudate and sloppy feeding (uningested food) all contribute to this process. Radioactivity was measured by liquid scintillation and corrected for background radioactivity. Quenching of samples was not detected.

1. Goldman, J. C. in *Flows of Energy and Materials in Marine Ecosystems* 1st edn, vol. 13 (ed. Fasham, M. J. R.) 137–170 (Plenum, New York, 1984).
2. Sheldon, R. W. Phytoplankton growth rates in the tropical ocean. *Limnol. Oceanogr.* **29**, 1342–1346 (1984).
3. Capblancq, J. Nutrient dynamics and pelagic food web interactions in oligotrophic and eutrophic environments: an overview. *Hydrobiologia* **207**, 1–14 (1990).
4. Harris, G. P. *Phytoplankton Ecology: Structure, Function and Fluctuation* 1st edn (Chapman and Hall, London, 1986).
5. Harris, G. P. Pattern, process and prediction in aquatic ecology. A limnological view of some general ecological problems. *Freshwat. Biol.* **32**, 143–160 (1994).
6. Wetzel, R. G. *Limnology* 2nd edn (Saunders, New York, 1983).
7. Hudson, J. J. & Taylor, W. D. Measuring regeneration of dissolved phosphorus in planktonic communities. *Limnol. Oceanogr.* **41**, 1560–1565 (1996).
8. *An Ecosystem Approach to Aquatic Ecology: Mirror Lake and its Environment* 1st edn (ed. Likens, G. E.) (Springer, New York, 1985).
9. Caraco, N. F., Cole, J. J. & Likens, G. E. New and recycled primary production in an oligotrophic lake: insights for summer phosphorus dynamics. *Limnol. Oceanogr.* **37**, 590–602 (1992).
10. Kraft, C. E. Phosphorus regeneration by Lake Michigan alewives in the mid-1970s. *Trans. Am. Fish. Soc.* **122**, 749–755 (1993).
11. Perezfuentetaja, A., McQueen, D. J. & Ramcharan, C. W. Predator-induced bottom-up effects in oligotrophic systems. *Hydrobiologia* **317**, 163–176 (1996).
12. Vanni, M. J. in *Food Webs: Integration of Patterns and Dynamics* 1st edn (eds Polis, G. A. & Winnemiller, K. O.) 81–95 (Chapman and Hall, New York, 1996).
13. Schaus, M. H. *et al.* Nitrogen and phosphorus excretion by detritivorous gizzard shad in a reservoir ecosystem. *Limnol. Oceanogr.* **42**, 1386–1397 (1997).
14. Horppila, J. *et al.* Top-down or bottom-up effects by fish: issues of concern in biomanipulation of lakes. *Restoration Ecol.* **6**, 20–28 (1998).
15. Nakashima, B. S. & Leggett, W. C. The role of fish in the regulation of phosphorus availability in lakes. *Can. J. Fish. Aquat. Sci.* **37**, 1540–1549 (1980).
16. den Oude, P. J. & Gulati, R. D. Phosphorus and nitrogen excretion rates of zooplankton from the eutrophic Loosdrecht lakes, with notes on other P sources for phytoplankton requirements. *Hydrobiologia* **169**, 379–390 (1988).
17. Mazumder, A. *et al.* Partitioning and fluxes of phosphorus: mechanisms regulating the size-distribution and biomass of plankton. *Arch. Hydrobiol. Beih.* **35**, 121–143 (1992).
18. Cyr, H. & Pace, M. L. Magnitude and patterns of herbivory in aquatic and terrestrial ecosystems. *Nature* **361**, 148–150 (1993).
19. Baines, S. B. & Pace, M. L. Relationship between suspended particulate matter and sinking flux along a trophic gradient and implications for the fate of planktonic primary production. *Can. J. Fish. Aquat. Sci.* **51**, 25–36 (1994).
20. Schindler, D. W. Evolution of phosphorus limitation in lakes. *Science* **195**, 260–262 (1977).
21. Edmondson, W. T. *The Uses of Ecology: Lake Washington and Beyond* 1st edn (Univ. Washington Press, Seattle, 1991).
22. Parsons, T. R., Maita, Y. & Lalli, C. M. *A Manual of Chemical and Biological Methods for Seawater Analysis* 1st edn (Pergamon, Oxford, 1984).
23. *Atlas of Alberta Lakes* 1st edn (eds Mitchell, P. & Prepas, E.) (Univ. of Alberta Press, Edmonton, 1990).
24. Lin, C. K. *Phytoplankton Succession in Astotin Lake, Elk Island National Park, Alberta* (Thesis, Univ. Alberta, Edmonton, 1968).
25. Gingras, B. A. & Paszkowski, C. A. Breeding patterns of common loons on lakes with three different fish assemblages in north-central Alberta. *Can. J. Zool.* (in the press).
26. *Prince Albert National Park Resource Description and Analysis* vol. 2 (Canadian Park Service) (Environment Canada, Parks, Prairie and Northern Region, Winnipeg, Manitoba, 1986).
27. Anderson, S. R. Crustacean plankton communities of 340 lakes and ponds in and near the national parks of the Canadian Rocky Mountains. *J. Fish. Res. Board. Can.* **31**, 855–869 (1974).
28. Ramcharan, C. W. *et al.* A comparative approach to determining the role of fish predation in structuring limnetic ecosystems. *Archiv. Hydrobiol.* **133**, 389–416 (1995).

Genome complexity, robustness and genetic interactions in digital organisms

Richard E. Lenski*, **Charles Ofria**†, **Travis C. Collier**‡ **& Christoph Adami**§

* *Center for Microbial Ecology, Michigan State University, East Lansing, Michigan 48824, USA*
† *Computation and Neural Systems and* § *Kellogg Radiation Laboratory, California Institute of Technology, Pasadena, California 91125, USA*
‡ *Department of Organismic Biology, Ecology, and Evolution, University of California, Los Angeles, California 90095, USA*

Digital organisms are computer programs that self-replicate, mutate and adapt by natural selection[1–3]. They offer an opportunity to test generalizations about living systems that may extend beyond the organic life that biologists usually study. Here we have generated two classes of digital organism: simple programs selected solely for rapid replication, and complex programs selected to perform mathematical operations that accelerate replication through a set of defined 'metabolic' rewards. To examine the differences in their genetic architecture, we introduced millions of single and multiple mutations into each organism and measured the effects on the organism's fitness. The complex organisms are more robust than the simple ones with respect to the average effects of single mutations. Interactions among mutations are common and usually yield higher fitness than predicted from the component mutations assuming multiplicative effects; such interactions are especially important in the complex organisms. Frequent interactions among mutations have also been seen in bacteria, fungi and fruitflies[4–6]. Our findings support the view that interactions are a general feature of genetic systems[7–9].

Many fundamental questions in biology are difficult to address, as a consequence of the high dimensionality of genomes[7–9] as well as the practical difficulties of manipulating numerous genotypes and analysing their resulting phenotypic properties. Progress has been made using microorganisms[4,5,10–18], but these problems remain daunting. An alternative approach involves studying artificial life,
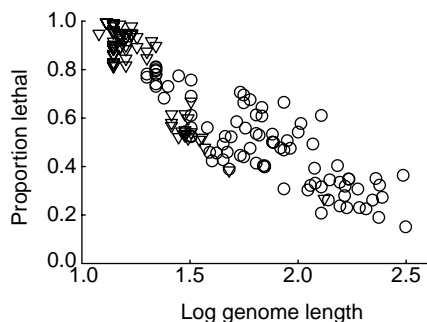
Figure 1 Proportion of single point mutations that are lethal for digital organisms. Shown as a function of $\log_{10}$-transformed genome length. Circles, complex organisms; triangles, simple organisms.
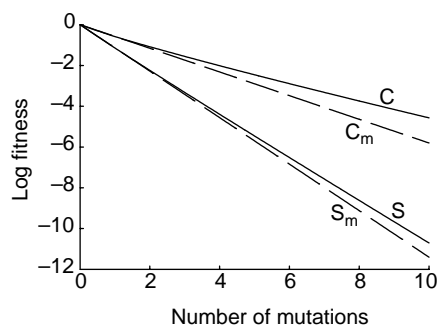

Figure 2 $\log_{10}$-transformed mean fitness as a function of number of point mutations for simple and complex classes of digital organisms. Solid curve C shows the fitness function calculated using the average parameter values from the complex organisms. Dashed line C_m is their fitness function expected under the multiplicative model (obtained using the average α and setting $\beta = 1$). Solid curve S is the fitness function for the average simple organism. Dashed line S_m gives the corresponding function expected under the multiplicative model.
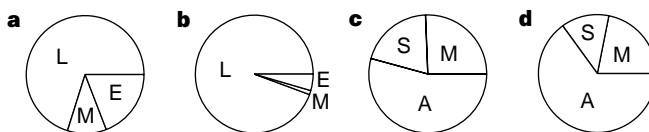

Figure 3 Proportions of mutational pairs classified according to their interaction. L, lethal: at least one mutation is lethal alone, as is the double mutant. M, multiplicative: neither mutation is lethal, and the relative fitness of the double mutant is exactly equal to the product of the relative fitnesses of the two single mutations. E, epistatic: the double mutant's fitness is unequal to the multiplicative expectation. S, synergistic: double mutant less fit than expected. A, antagonistic: the double mutant is more fit than expected. Average distributions are for complex organisms (**a**), simple organisms (**b**), complex excluding lethals (**c**), and simple excluding lethals (**d**).

Table 1 Comparisons between complex and simple digital organisms of genome size and several mutational-effect parameters

Response variable	Mean complex (± s.d.)	Mean simple (± s.d.)	Mean difference (± s.d.)	P*
Genome length	91.25 (69.07)	19.80 (14.18)	71.45 (64.76)	<0.0001
Decay test, α	0.581 (0.207)	1.141 (0.591)	−0.560 (0.562)	<0.0001
Decay test, β	0.896 (0.081)	0.972 (0.192)	−0.077 (0.201)	0.0011
Pair test, proportion epistatic of total	0.191 (0.093)	0.045 (0.080)	0.146 (0.122)	<0.0001
Pair test, proportion epistatic of non-lethal	0.743 (0.243)	0.781 (0.234)	−0.038 (0.303)	0.4374
Pair test, proportion synergistic of epistatic	0.271 (0.093)	0.168 (0.159)	0.103 (0.175)	<0.0001

* Two-tailed Wilcoxon signed-ranks test of the differences between 87 paired complex and simple organisms.

in particular certain computer programs—or digital organisms—that share with real organisms the properties of self-replication, mutation, competition and evolution, as well as genomes with high dimensionality and hence indeterminate evolutionary trajectories. The use of digital organisms to address biological questions is controversial, but it can be justified on several grounds. First, artificial life allows us to seek generalizations beyond the organic forms that biologists have studied to date, all of which derive from a common ancestor and share the same basic chemistry of DNA, RNA and proteins. Maynard Smith makes the case thus[19]: "So far, we have been able to study only one evolving system and we cannot wait for interstellar flight to provide us with a second. If we want to discover generalizations about evolving systems, we will have to look at artificial ones." Second, digital organisms allow us to perform experiments on a scale that is unattainable with real organisms. Here we test billions of different genotypes to measure mutational effects and interactions; a recent experiment with the bacterium *Escherichia coli* did so using a few hundred genotypes[4]. Moreover, the performance of digital organisms can be measured exactly, whereas such data are subject to error, and hence loss of statistical power, in any real biological system. Third, there is growing interest in using programs that can evolve to solve complex computational problems[20–23]. Knowing how mutations affect performance and interact with one another has important implications for setting parameters such as mutation and recombination rates, just as mutational effects and interactions can influence the evolution of these parameters in real organisms[4,6,24–28].

Our experiments were performed using Avida, a flexible platform for research on artificial life[3]. Briefly, digital organisms are self-replicating computer programs that compete for central processing unit (CPU) time, which is the fuel needed for their replication. The programs mutate at random and evolve in a defined computational environment. Each digital organism has a genome length measured as the number of sequential instructions in its program. The sequence of instructions can change by mutation, including insertion and deletion events as well as point mutations that change one instruction to another. There are 28 different instructions, which can be thought of as analogous to the 20 different amino acids strung together in proteins. There is no imposed limit to the genome length of these digital organisms.

Starting from a short ancestral program, we generated 87 different 'complex' organisms by allowing replicated populations to evolve in an environment in which: (1) the baseline allocation of CPU time is proportional to genome size; and (2) certain mathematical operations, which require novel combinations of instructions, are rewarded with additional CPU time. For example, digital organisms may be rewarded for performing an 'XOR' operation ('exclusive-or' in which A or B is true, but not both) on 32-bit inputs using a series of 'NAND' operations ('not-and' in which A and B are not simultaneously true). 'XOR' is among the more complicated logical operations; 'NAND' is the only logical operator given as an instruction in Avida. In essence, these operations are a kind of metabolism that allows the digital organisms to acquire the CPU time needed for their replication. Starting from each complex organism, we derived a 'simple' organism that evolved in an environment that favoured faster replication and nothing else: (1) the allocation of CPU time is independent of genome length; and (2) mathematical operations are not rewarded. Thus, we define simple and complex organisms by the different environments in which they evolved. However, we cannot exclude the possibility that aspects other than functional complexity might contribute to differences between the two classes; for example, relaxed selection

for genome size in complex organisms may promote genetic redundancy, with attendant consequences for mutational effects.

All 87 simple digital organisms have shorter genomes than their paired complex progenitors, with mean lengths of 19.8 and 91.3 instructions, respectively (Table 1). In every case, both simple and complex digital organisms became more fit than their progenitors in their respective environments, where fitness is simply an organism's replication rate. Using all 174 complex and simple organisms, we then performed two experiments to investigate the effects of mutations and their interactions with respect to fitness. In the first experiment—the 'decay test'—we generated, for each organism, every possible mutant program that contained exactly one point mutation, plus a million (or more) programs with between two and ten random mutations. For each mutant, we measured fitness relative to its unmutated parent in the parent's selective environment. Then, for each parent, we regressed the average mutant fitness W versus mutation number M using a power function: $\log_{10} W = -\alpha M^\beta$. In biological terms, α describes the rate at which fitness decays under a multiplicative hypothesis, whereas β describes the form of 'epistasis'. If $\beta = 1$, mutational effects are multiplicative; if $\beta > 1$, each successive mutation tends to reduce fitness more than previous ones (synergistic epistasis); and if $\beta < 1$, each additional mutation is progressively less damaging on average (antagonistic epistasis). The parameter α is measured without error because $W = 1$ when $M = 0$ (by definition) and every possible mutant with $M = 1$ is tested, whereas β is estimated from sample data. The power function fits these data very well; unlike a quadratic function[4], it never predicts that the decay curve bends upwards at high M.

Simple organisms are much more fragile than their complex counterparts with respect to the fitness effects of single mutations, as indicated by higher values of α ($P < 0.0001$; Table 1). This difference occurs because more mutations are lethal (prevent self-replication) in smaller genomes than in larger genomes (Fig. 1); on average, 92% and 53% of single mutations were lethal to simple and complex organisms, respectively. Partly offsetting this effect, non-lethal mutations are less damaging to the simple digital organisms; one non-lethal mutation reduces fitness by 11%, on average, in simple organisms, but by 44% in complex ones. The simple organisms do nothing except self-replicate; mutations that disrupt self-replication tend to be lethal, whereas most others are fairly harmless. The complex organisms perform mathematical functions in addition to self-replicating; most mutations that impact these functions hinder performance but are not lethal.

Simple and complex digital organisms also differ in terms of β, which indicates the average form of interaction ($P = 0.0011$; Table 1). In complex organisms, successive mutations tend to reduce fitness less than would be expected if effects were independent ($\beta < 1$), that is, complex organisms are also robust to the cumulative effect of multiple mutations. By contrast, successive mutations do not deviate significantly from multiplicative effects ($\beta = 1$) in simple organisms ($P = 0.2360$, Wilcoxon signed-ranks test). Figure 2 shows the difference between simple and complex digital organisms in their fitness decay curves, including the effects of both α and β.

The fact that simple organisms appear to show multiplicative effects of mutations on average fitness may mean either that there is little epistasis or that epistasis is widespread but different sets of mutations interact in opposite ways, obscuring the overall signal[4,27]. We ran a second experiment—the 'pair test'—to distinguish between these two possibilities and gain further insight into the differences between simple and complex organisms. Instead of measuring fitness as progressively more mutations are added, as in the decay test, we examined numerous pairs of mutations by comparing the actual fitness of each double mutant with the expected fitness assuming multiplicative effects of the component mutations. The pair test shows that epistasis is more common in complex organisms than in their simple counterparts ($P < 0.0001$; Table 1), with 19% of all mutation pairs deviating from multiplicative effects in the average complex organism (Fig. 3a) compared with $<5\%$ in the average simple organism (Fig. 3b). Frequencies of epistatic interactions are much higher if we exclude lethal pairs, in which actual and expected fitnesses are both zero (Fig. 3c, d). Excluding lethal pairs, which are much more common in simple organisms, there is no difference between classes in the prevalence of epistasis ($P = 0.4374$; Table 1). In both classes of digital organisms, epistatic interactions include a mixture of synergistic and antagonistic effects, and antagonistic effects are more common than synergy. Complex organisms are more prone to synergistic effects when expressed as a percentage of epistatic interactions ($P < 0.0001$; Table 1), but the overall excess of antagonism is greater in complex organisms. The failure of the decay test to find a significant deviation from multiplicative effects in the simple organisms evidently reflects a combination of two factors: epistasis is infrequent, and synergistic and antagonistic interactions oppose one another.

In summary, mutations in digital organisms frequently exhibit epistasis, including a diverse mixture of synergistic and antagonistic interactions. Such interactions are especially pronounced in the complex digital organisms that evolved large genomes and are rewarded for mathematical operations beyond self-replication. Frequent epistasis, including a mix of synergistic and antagonistic effects, also exists in a variety of real organisms[4-6]. Thus, digital organisms experience complicated responses to genetic perturbations that appear similar to those seen in real organisms. The genomes and performances of digital organisms can be studied with far greater replication and precision than can be achieved with any real organism. Digital organisms may therefore offer a useful tool for addressing other biological questions in which complexity is both a barrier to understanding and an essential feature of the whole living system. Moreover, digital organisms allow us to test general hypotheses with a system that is built upon an artificial chemistry completely different from that used by real organisms. □

Methods

Evolution of digital organisms. Experiments were performed using version 1.3 of Avida, which can be obtained from http://www.krl.caltech.edu/avida/pubs/nature99. We used default settings unless otherwise indicated. Our first step was to generate pairs of complex and simple organisms. All evolution experiments began with the population at its carrying capacity (3,600 individuals). The probability of point mutation was 0.0075 per instruction copied; the probabilities of insertion and deletion mutations were each 0.05 per genome divide. Time is measured in arbitrary units called updates; every update represents the execution of an average of 30 instructions per individual in the population. (A typical generation is 5–10 updates, depending on genome size and execution.) Starting with the default ancestor (genome length 20), a population of complex organisms was propagated for 50,000 updates in an environment in which the baseline allocation of CPU time was proportional to genome size and extra CPU time was obtained by performing mathematical operations in the default task set. The former condition eliminates selection for smaller genomes, and the latter condition imposes selection for functional complexity. The rewards for performing operations are also specified in the default task set; they are scaled by their approximate difficulty and combined in a multiplicative fashion with one another and with the baseline CPU time. (Note that multiplicative scaling of phenotypic rewards does not imply multiplicative effects of mutations.) Using random number seeds, 87 complex populations were derived; subsequent experiments used the numerically dominant genotype from each population. Starting with each complex organism as progenitor, a population of simple organisms evolved for 25,000 updates by allocating the same CPU time to all organisms. There was selection for smaller genome size to promote faster replication and no selection for mathematical operations. Subsequent experiments used the most abundant genotype from each population.

Mutational analyses. We developed three genetic tools to analyse the effects of

point mutations on the performance of digital organisms. In all cases, the fitness (replication rate) of each mutant was calculated in the same environment in which its simple or complex parent evolved, and the mutant's fitness is expressed relative to the parent. The first tool makes every possible one-step point mutant for a particular parent. The default set includes 28 different instructions; given a parent of genome length 80, for example, there are $80 \times (28 - 1) = 2,160$ different one-step point mutants. The mean fitness of these mutants permits exact calculation of α in the decay test. The second tool produces a random sample of progeny that differ from their parent by two or more point mutations. For each parent, we generated between 10^5 and 10^7 progeny with two mutations, three mutations and so on, up to ten mutations. The third tool produces and analyses pairs of point mutations alone and in combination; for each two-step mutant, we have both corresponding one-step mutants. Having the single mutants allows us to compare a double mutant's actual fitness with the exact value expected under the hypothesis that the mutations interact in a multiplicative manner. We ran the pair test on 10^4 and 10^5 mutational pairs for each complex and simple organism, respectively.

Statistical methods. We performed the Wilcoxon signed-ranks test on the difference scores for all comparisons between complex and simple organisms[29]. This test reflects the evolutionary relationship between pairs of organisms; it is also non-parametric and thus insensitive to deviations from a normal distribution. To estimate β in the decay tests, we minimized the sum of squared deviations around the log-transformed mean fitness values. We excluded samples with fewer than 100 viable mutants, in which case log mean fitness was poorly estimated. By increasing sample size to 10^8, we can obtain additional viable mutants; the exclusion of some values because of insufficient sampling appears to have no systematic effect on estimation of β.

1. Ray, T. S. in *Artificial Life II* (eds Langton, C. G., Taylor, C., Farmer, J. D. & Rasmussen, S.) 371–408 (Addison-Wesley, Redwood City, California, 1991).
2. Adami, C. Learning and complexity in genetic auto-adaptive systems. *Physica D* **80,** 154–170 (1995).
3. Adami, C. *Introduction to Artificial Life* (Springer, New York, 1998).
4. Elena, S. F. & Lenski, R. E. Test of synergistic interactions among deleterious mutations in bacteria. *Nature* **390,** 395–398 (1997).
5. De Visser, J. A. G. M., Hoekstra, R. F. & van den Ende, H. Test of interaction between genetic markers that affect fitness in *Aspergillus niger. Evolution* **51,** 1499–1505 (1997).
6. Clark, A. G. & Wang, L. Epistasis in measured genotypes: *Drosophila* P-element insertions. *Genetics* **147,** 157–163 (1997).
7. Wright, S. *Evolution and the Genetics of Populations* (Univ. Chicago Press, 1977).
8. Kauffman, S. & Levin, S. Towards a general theory of adaptive walks on rugged landscapes. *J. Theor. Biol.* **128,** 11–45 (1987).
9. Kauffman, S. A. *The Origins of Order* (Oxford Univ. Press, New York, 1993).
10. Paquin, C. & Adams, J. Relative fitness can decrease in evolving populations of *S. cerevisiae. Nature* **306,** 368–371 (1983).
11. Dykhuizen, D. E., Dean, A. M. & Hartl, D. L. Metabolic flux and fitness. *Genetics* **115,** 25–31 (1987).
12. Lenski, R. E. & Travisano, M. Dynamics of adaptation and diversification: a 10,000-generation experiment with bacterial populations. *Proc. Natl Acad. Sci. USA* **91,** 6808–6814 (1994).
13. Rosenzweig, R. F., Sharp, R. R., Treeves, D. S. & Adams, J. Microbial evolution in a simple unstructured environment: genetic differentiation in *Escherichia coli. Genetics* **137,** 903–917 (1994).
14. Travisano, M., Mongold, J. A., Bennett, A. F. & Lenski, R. E. Experimental tests of the roles of adaptation, chance, and history in evolution. *Science* **267,** 87–90 (1995).
15. Rainey, P. B. & Travisano, M. Adaptive radiation in a heterogeneous environment. *Nature* **394,** 69–72 (1998).
16. Burch, C. L. & Chao, L. Evolution by small steps and rugged landscapes in the RNA virus φ6. *Genetics* **151,** 921–927 (1999).
17. De Visser, J. A., Zeyl, C. W., Gerrish, P. J., Blanchard, J. L. & Lenski, R. E. Diminishing returns from mutation supply rate in asexual populations. *Science* **283,** 404–406 (1999).
18. Turner, P. E. & Chao, L. Prisoner's dilemma in an RNA virus. *Nature* **398,** 441–443 (1999).
19. Maynard Smith, J. Byte-sized evolution. *Nature* **335,** 772–773 (1992).
20. Holland, J. H. *Adaptation in Natural and Artificial Systems* (MIT Press, Cambridge, Masachusetts, 1992).
21. Koza, J. R. *Genetic Programming* (MIT Press, Cambridge, Massachusetts, 1992).
22. Frank, S. A. in *Adaptation* (eds Rose, M. R. & Lauder, G. V.) 451–505 (Academic, New York, 1996).
23. Koza, J. R., Bennett, F. H., Andre, D. & Keane, M. A. in *Evolutionary Robotics* (ed. Gomi, T.) 37–76 (AAI Press, Kanata, Canada, 1998).
24. Maynard Smith, J. *The Evolution of Sex* (Cambridge Univ. Press, 1978).
25. Kondrashov, A. S. Deleterious mutations and the evolution of sexual reproduction. *Nature* **336,** 435–440 (1988).
26. Hurst, L. D. & Peck, J. R. Recent advances in understanding of the evolution and maintenance of sex. *Trends Ecol. Evol.* **11,** 46–52 (1996).
27. Otto, S. P. & Feldman, M. W. Deleterious mutations, variable epistatic interactions, and the evolution of recombination. *Theor. Popul. Biol.* **51,** 134–147 (1997).
28. Eyre-Walker, A. & Keightley, P. D. High genomic deleterious mutation rates in hominids. *Nature* **397,** 344–347 (1999).
29. Sokal, R. R. & Rohlf, F. J. *Biometry* 3rd edn (Freeman, New York, 1994).

A general model for the structure and allometry of plant vascular systems

Geoffrey B. West*†, **James H. Brown**†‡ & **Brian J. Enquist**†‡

* *Theoretical Division, T-8, MS B285, Los Alamos National Laboratory, Los Alamos, New Mexico 87545, USA*
† *The Santa Fe Institute, 1399 Hyde Park Road, Santa Fe, New Mexico 87501, USA*
‡ *Depatment of Biology, University of New Mexico, Albuquerque, New Mexico 87131, USA*

Vascular plants vary in size by about twelve orders of magnitude, and a single individual sequoia spans nearly this entire range as it grows from a seedling to a mature tree. Size influences nearly all of the structural, functional and ecological characteristics of organisms[1,2]. Here we present an integrated model for the hydrodynamics, biomechanics and branching geometry of plants, based on the application of a general theory of resource distribution through hierarchical branching networks[3] to the case of vascular plants. The model successfully predicts a fractal-like architecture and many known scaling laws, both between and within individual plants, including allometric exponents which are simple multiples of 1/4. We show that conducting tubes must taper

---

Box 1 Notation and geometry

The model can be described as a continuously branching hierarchical network running from the trunk (level 0) to the petioles (level N), with an arbitrary level denoted by k (Fig. 1). The architecture is characterized by three parameters (a, $\bar{a}$ and n), which relate daughter to parent branches: ratios of branch radii, $\beta_k \equiv r_{k+1}/r_k \equiv n^{-a/2}$, tube radii, $\bar{\beta}_k \equiv a_{k+1}/a_k \equiv n^{-\bar{a}/2}$, and branch lengths, $\gamma_k \equiv l_{k+1}/l_k$ and also the branching ratio, n, the number of daughter branches derived from a parent branch. Because the total number of tubes is preserved at each branching, $n = n_{k+1}/n_k$, where n_k is the number of tubes in a kth-level branch; n is taken to be independent of k and typically equals 2. Clearly, $n_k = n_N n^{N-k}$, where N is the total number of branching generations from trunk to petiole, and n_N is the number of tubes in a petiole, which is taken to be an invariant. Now, for a volume-filling network, $\gamma_k = n^{-1/3}$, independent of k (ref. 3). If tube tapering is uniform, $\bar{a}$ is also independent of k, and it follows that

$$\frac{r_k}{r_N} = n^{(N-k)a/2}; \quad \frac{a_k}{a_N} = \left(\frac{r_k}{r_N}\right)^{\bar{a}/a}; \quad \frac{l_k}{l_N} = \left(\frac{r_k}{r_N}\right)^{2/3a} \quad (1)$$

Various scaling laws can now be derived. For example, the number of terminal branches or leaves distal to the kth branch, $n_k^L = n_k/n_N = n^{N-k} = (r_k/r_N)^{2/a}$, and the area of conductive tissue (CT), $A_k^{CT} = n_k \pi a_k^2 = A_N^{CT}(r_k/r_N)^{2(1+\bar{a})/a}$, where $A_N^{CT} = n_N \pi a_N^2$ is the area of conductive tissue in a petiole. Thus, the area of conductive tissue relative to the total (tot) branch cross-sectional area ($A_k^{tot} = \pi r_k^2$) is given by

$$f_k \equiv \frac{A_k^{CT}}{A_k^{tot}} = n_N \left(\frac{a_N^2}{r_N^2}\right)\left(\frac{r_k}{r_N}\right)^{2(1+\bar{a}-a)/a} \quad (2)$$

The total cross-sectional area scales as $n A_{k+1}^{tot}/A_k^{tot} = n\beta_k^2 = n^{1-a}$. When $a = 1$ this reduces to unity and the branching is area-preserving; that is, the cross-sectional area of the daughter branches is equal to that of the parent: $n A_{k+1}^{tot} = A_k^{tot}$. A simple example of this, considered in ref. 3, is the pipe model[6], in which all tubes have the same constant diameter ($\bar{a} = 0$), are tightly bundled and have no non-conducting tissue. Here we consider the more realistic case in which tubes are loosely packed in sapwood and there may be non-conducting heartwood providing additional mechanical stability.